

# The Use of Genetic Algorithms in Multilayer Mirror Optimization

by

Shannon Lunt

March 1999

Submitted to Brigham Young University in partial fulfillment of graduation requirements for University Honors

Advisor: R. Steven Turley Honors Dean: Steven E. Benzley

Signature: \_\_\_\_\_ Signature: \_\_\_\_\_

# Contents

|          |   |           |
|----------|---|-----------|
| <b>1</b> | <b>Introduction</b>   | <b>5</b>  |
| 1.1      | Interest in the XUV Region . . . . .                              | 5         |
| 1.2      | IMAGE Mission—XUV and Specifications . . . . .                    | 6         |
| 1.3      | Optimization Techniques . . . . .                                 | 7         |
| 1.3.1    | Local Optimizers . . . . .  | 8         |
| 1.3.2    | Global Optimizers . . . . .                                       | 9         |
| 1.4      | Calculation of Reflectivities . . . . .                           | 9         |
| 1.5      | Reflectivity of X Rays . . . . .                                  | 11        |
| 1.6      | A New Application of the GA . . . . .                             | 14        |
| 1.7      | Outline . . . . .   | 14        |
| <b>2</b> | <b>Genetic Algorithm</b>  | <b>15</b> |
| 2.1      | Description . . . . .   | 15        |
| 2.2      | Advantages and Disadvantages for this Class of Problems . . . . . | 17        |
| 2.3      | The GA Applied to the IMAGE Mission . . . . .                     | 17        |
| 2.3.1    | Materials and Thicknesses . . . . .                               | 18        |
| 2.3.2    | Study of Seeds . . . . .  | 18        |
| 2.3.3    | Selecting Parents and Reproduction . . . . .                      | 20        |
| 2.3.4    | Merit Function . . . . .  | 23        |
| 2.3.5    | Hybrid Used . . . . .   | 24        |
| <b>3</b> | <b>Results</b>  | <b>26</b> |
| 3.1      | Mirrors Designed for the IMAGE Mission . . . . .                  | 26        |
| 3.2      | Periodic and Aperiodic Designs . . . . .                          | 28        |
| 3.3      | Diagnostics . . . . .   | 30        |
| 3.4      | Polarizers . . . . .  | 31        |
| 3.5      | Selection of Parameters . . . . .                                 | 31        |
| 3.5.1    | Study of Population Size (N) . . . . .                            | 32        |
| 3.5.2    | Optimal Parameters . . . . .                                      | 35        |
| <b>4</b> | <b>Conclusion</b>   | <b>36</b> |
| 4.1      | Where the GA is Valuable . . . . .                                | 36        |
| 4.2      | Rules for Application of the GA . . . . .                         | 36        |
| 4.3      | Future Research . . . . .   | 37        |

## List of Figures

|    |  |    |
|----|--|----|
| 1  | Graph of a one-dimensional solution space . . . . .  | 7  |
| 2  | Diagram of Snell's Law . . . . .                     | 10 |
| 3  | Multiple reflections from multilayers . . . . .      | 12 |
| 4  | Geometry for the Parratt recursion formula . . . . . | 13 |
| 5  | Composition of the Chromosomes . . . . .             | 15 |
| 6  | Flow chart of the Genetic Algorithm . . . . .        | 16 |
| 7  | Crossover of the Genes . . . . .                     | 22 |
| 8  | Mutation of the Genes . . . . .                      | 22 |
| 9  | Reflectivity of $Y_2O_3/Al$ at 304 Å. . . . .        | 26 |
| 10 | Reflectivity of $Y_2O_3/Al$ at 584 Å. . . . .        | 26 |
| 11 | Reflectivity of $U/Si$ at 304 Å. . . . .             | 27 |
| 12 | Reflectivity of $U/Si$ at 584 Å. . . . .             | 27 |
| 13 | Reflectivity of $Mo/Si$ at 304 Å. . . . .            | 28 |
| 14 | Reflectivity of $Mo/Si$ at 584 Å. . . . .            | 28 |
| 15 | Reflectivity of periodic $U/Al$ at 304 Å. . . . .    | 29 |
| 16 | Reflectivity of periodic $U/Al$ at 584 Å. . . . .    | 29 |
| 17 | Reflectivity of aperiodic $U/Al$ at 304 Å. . . . .   | 30 |
| 18 | Reflectivity of aperiodic $U/Al$ at 584 Å. . . . .   | 30 |
| 19 | Convergence of GA. . . . .                           | 35 |

## List of Tables

|    |   |    |
|----|---|----|
| 1  | Terminology in the GA . . . . .                                   | 17 |
| 2  | Parameters specific to each application of the GA . . . . .       | 18 |
| 3  | Study of 4 layer mirrors designed with different seeds . . . . .  | 19 |
| 4  | Study of 10 layer mirrors designed with different seeds . . . . . | 19 |
| 5  | Study of 16 layer mirrors designed with different seeds . . . . . | 20 |
| 6  | 16 layers on $SiO_2$ with a population of 6000 . . . . .          | 24 |
| 7  | 16 layers on $SiO_2$ with a population of 6000 . . . . .          | 25 |
| 8  | Study of 4 layer mirrors with different populations . . . . .     | 32 |
| 9  | Study of 10 layer mirrors with different populations . . . . .    | 33 |
| 10 | Study of 14 layer mirrors with different populations . . . . .    | 34 |

## **Abstract**

This paper describes the genetic algorithm applied to multilayer mirror optimization. An explanation of how genetic algorithms work is given and how this algorithm was applied to the design of bifunctional mirrors for the IMAGE Mission.

This paper also discusses some findings that contradict previous design rules for multilayer mirrors. Some of these are: aperiodic mirrors performing better than periodic mirrors and an oxide producing a better design than a mirror with just elements as materials.

Using the genetic algorithm, the best mirror design found for the IMAGE Mission was an aperiodic  $\text{Y}_2\text{O}_3/\text{Al}$  16 layer stack on  $\text{SiO}_2$ . This design had a predicted reflectivity of 36% at 304 Å and .2% at 584 Å.

# 1 Introduction

## 1.1 Interest in the XUV Region

Much is known about the physics of the interaction of radiation with matter in the extreme ultraviolet (XUV) or soft x-ray region. Some applications are developing that take advantage of what is currently known and extend the understanding of this region. To image an object, light with a wavelength less than the size of the object must be used. Since most cells are on the order of a micrometer in size, soft x-rays, which are on the order of hundreds of angstroms ( $\text{\AA}$ ), can be used to “see” these objects. In the past, high resolution microscopy has been used to image cells but it requires killing the sample. Soft x-ray microscopy can image live objects, allowing dynamic imaging of evolving cellular processes. There is also an interest in using the XUV in photolithography. If shorter wavelengths (about  $130\text{\AA}$ ) are used in microelectronic circuits, one can make smaller circuits that work at a lower temperature and are much faster and more dense than current circuits. With smaller circuits, less charge would be needed by each circuit so the temperature would be lower and the total power used would be less.

Research in the XUV region is also important because there is a lot of contradictory and missing data about the index of refraction of many materials in this region. This is partly due to the energies in this region being comparable to that of atomic bonds in solids. As more is learned about the index of refraction of various materials, the understanding of what is going on in the materials increases.

By the Kramers-Kronig relation, if the index of refraction for a material is known at one wavelength, then the information at all wavelengths can be calculated. This information tells about the real and imaginary parts of the index of refraction and fills in the gaps in current data. The Kramers-Kronig relation connects the real and imaginary parts of the atomic scattering factor,  $f$ , where  $f'$  is the real part and  $f''$  is the imaginary part:

$$f''(\omega) = \frac{2}{\pi} \int_0^{\infty} \frac{\omega' f''(\omega') d\omega'}{\omega^2 - \omega'^2}. \quad (1)$$

In Equation 1,  $\omega$  is the frequency of the incident wave and  $\omega'$  is the natural resonance frequency [1]. It is possible to calculate  $f''$  from crystals and then  $f'$  can be found using this relation. The real and imaginary parts of the atomic scattering factor are connected to the real and imaginary parts of the index of refraction,  $\tilde{n} = n + i\kappa$ , as follows:

$$n = 1 - \frac{N\lambda^2}{2\pi} \frac{e^2}{mc^2} f' \quad (2)$$

$$\kappa = \frac{N\lambda^2}{2\pi} \frac{e^2}{mc^2} f'', \quad (3)$$

where  $N$  is the number of atoms per cubic centimeter,  $\lambda$  is the wavelength of light in vacuum,  $e$  is the charge of an electron,  $m$  is the mass of an electron, and  $c$  is the speed of light in vacuum [2]. The complex index of refraction is discussed in Section 1.5. From this relation, if  $f'$  and  $f''$  are known at one wavelength, the index of refraction can be calculated. This knowledge is very useful in XUV astronomy because the radiation from stars at different wavelengths tells us different things about the star. In this region, information can be obtained about the inner parts of the star where the fusion reactions take place.

## 1.2 IMAGE Mission—XUV and Specifications

Another application in the XUV and the topic of this paper was to design a mirror for the XUV section of the IMAGE Mission which will be launched in January 2000 and whose goal is to image the magnetosphere. The mirror was specified at 14.5 degrees from normal to be highly reflective ( $> 20\%$ ) at 304 Å to see the He-II lines from the magnetosphere and to be non-reflective ( $< .2\%$ ) at 584 Å to cut out the bright He-I lines from the earth's atmosphere which would saturate the detector.

This project was accepted because it was already known how to design a highly reflective mirror at one wavelength. Since 584 Å is just a little over twice as long as 304 Å, it was thought that the same mirrors that were highly reflective at 304 Å could also be non-reflective at 584 Å. Through the course of the project, this was found to be a difficult problem because most materials are more

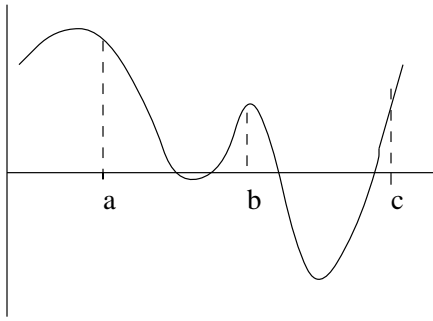


Figure 1: Graph of a one-dimensional solution space

reflective at  $584 \text{ \AA}$  than at  $304 \text{ \AA}$ . Also, aperiodic stacks, multilayer mirrors with each layer having a different thickness, were found to produce better mirrors for this problem than periodic mirrors did, contrary to most previous knowledge [4]. A discussion of why multilayer mirrors are used in the XUV regions is included in Section 1.5. By using aperiodic stacks, though, another problem arises as there is a huge space to search for a solution and there are many parameters to fit (each layer thickness and possibly the materials).

### 1.3 Optimization Techniques

When there is a problem with one or more independent variables, it is often desirable to maximize or minimize a characteristic merit function, otherwise known as optimization. The location of a maximum or minimum is found and then the maximum or minimum value of the function is calculated. The solution space for a function to be optimized can be represented two-dimensionally as in Figure 1. If one only looks between points  $a$  and  $b$  in the figure, a minimum will be found but it is only a local minimum. From the figure one can see that there is a deeper minimum between points  $b$  and  $c$ . Since this is the point with the lowest value for the function in the solution space, this is the global minimum.

Optimization techniques utilize information about the problem which is encoded in a merit

function. As the function is changed in the search for a maximum or minimum, the merit function is recalculated and tells how good the solution is. Thus, if one is searching for a minimum, the best solution will have the highest or lowest merit function.

### 1.3.1 Local Optimizers

Local optimization procedures take advantage of the decrease in value of the function near a minimum to converge to a solution. Thus, if the initial starting point is near a local minimum, that will be the solution found and there is no way of knowing about or finding better solutions. Two types of local optimizers use different approaches to take steps in the solution space: those that find the direction in which the value of the function is decreasing by blind searching and those that use information about the gradient of the solution space at a point to find a minimum.

An example of this first type and one of the simplest optimization techniques is the downhill simplex method developed by Nelder and Mead and explained in *Numerical Recipes*[10]. The solution space is encoded into a simplex—a multidimensional shape. An initial guess is given and at each step in the process, one of the sides of the simplex is extended, contracted, or reflected through another side to find a minimum value. Successive steps lead to a local minima by following the direction of decreasing value. The algorithm terminates when the step taken is smaller than a tolerance defined or the decrease in the function value at the last step is smaller than a certain tolerance. This method can be compared to someone walking in a dark cave high up in a mountain. He will feel in different directions with his feet until he finds the step that will take him lower. He then follows this method until he cannot go any lower and hopefully he has made it out of the mountain. Unfortunately, one can get stuck in a local minima, which is not the global minima. Although this method has no allowance for fixing this problem and has to have an initial point in the space given to it, it is very simple to apply.

The second type of local optimization requires the computation of derivatives. An example of this is the conjugate gradient method [10]. This approach allows one to find a local minimum quickly



with the calculation of the gradient and one-dimensional sub-minimization. An initial point is chosen and the gradient is computed. Then the conjugate to this gradient is found and the direction is followed while the function is decreasing. This is repeated until a local minimum is found. The conjugate gradient method has relatively fast convergence but is not very useful when the derivative of the function to be optimized is difficult to calculate or does not exist.

The simplex and conjugate gradient methods are both local optimization techniques. These methods do not handle discrete variables, discontinuities in solutions, or parameter constraints well. In optimizing a function, one wants the best solution or global extreme rather than a local extreme. Also, as in the project described in Section 1.2, the function to be optimized often includes discrete variables, represented by the material choices, and parameter constraints, represented by a minimum thickness being set for each layer in the mirror.

### **1.3.2 Global Optimizers**

A global optimizer is one which samples most of the solution space and is more apt to find the global extreme rather than just a local extreme. Global optimization procedures such as simulated annealing [8, 9] and genetic algorithms [3] are able to handle these difficulties well and are less sensitive to an initial guess. These global techniques begin with a random initialization and converge to a solution through a sequence of structured changes in the parameters. The randomness in movements and in the initial population allow global extrema to be found but make these methods inherently very time intensive.

## **1.4 Calculation of Reflectivities**

Each step in the process of optimizing a mirror design requires the calculation of the reflectivity, which is used in the merit function. In calculating reflectivities when using an unpolarized source, one must take into account two different polarizations of light as determined by the direction of the electric (E) field. As shown in Figure 2, s polarization is when the E-field is perpendicular to the

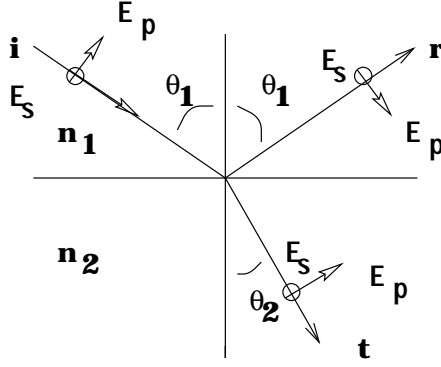


Figure 2: Diagram of Snell's Law

plane of incidence created by the incident and reflected waves, and  $p$  polarization is when the E-field is parallel to the plane of incidence. When light reaches a boundary, some of the light is reflected and some is transmitted. Snell's law relates the incident and transmitted angles in Equation 4, where  $n$  is the index of refraction of the material. This is also shown in Figure 2.

$$n_1 \sin \theta_1 = n_2 \sin \theta_2 \quad (4)$$

With a complex index of refraction, the angle of reflection,  $\theta$ , is also complex and no longer represents a geometrical angle.

The Fresnel equations [7] give a relation for finding the coefficients for light of  $s$  and  $p$  polarization. When combined with Snell's law they give Equations 5 and 6, where  $n = n_2/n_1$  and  $\theta$  is the angle between the incident wave and the normal to the plane, or  $\theta_1$  in Figure 2:

$$r_s = \frac{\cos \theta - \sqrt{n^2 - \sin^2 \theta}}{\cos \theta + \sqrt{n^2 - \sin^2 \theta}} \rightarrow \frac{n_1 - n_2}{n_1 + n_2} \text{ at } \theta = 0 \quad (5)$$

$$r_p = \frac{-n^2 \cos \theta + \sqrt{n^2 - \sin^2 \theta}}{n^2 \cos \theta + \sqrt{n^2 - \sin^2 \theta}} \rightarrow \frac{n_1 - n_2}{n_1 + n_2} \text{ at } \theta = 0. \quad (6)$$

Equations 4 and 5 allow the reflectivities to be calculated due to the  $s$  and  $p$  polarizations from the Fresnel coefficients,  $r_s$  and  $r_p$ :

$$R_s = |r_s|^2 \quad (7)$$

$$R_p = |r_p^2|. \quad (8)$$

If an unpolarized source and detector are used in the experiment, the total reflection can be found by combining the reflectivities due to the two different polarizations:

$$R = \frac{R_s + R_p}{2}. \quad (9)$$

## 1.5 Reflectivity of X Rays

Although the wavelength of light in the XUV region is much shorter than for visible light (hundreds of Å's compared to hundreds of nanometers), the same equations can be used in calculating reflectivities. In the XUV region, though, the index of refraction,  $n$ , becomes complex and is very close to one. This complex index of refraction can be represented as  $\tilde{n} = n + i\kappa$ , where  $n$  is the real part of the index of refraction and  $\kappa$  is the absorption constant.

A plane wave can be represented by

$$E = E_0 e^{i(\vec{k} \cdot \vec{r} - \omega t + \phi)}, \quad (10)$$

where  $k$  is the wave number and  $E_0$  is the amplitude of the wave. The definition of the wave number says that  $k_0 = \frac{2\pi}{\lambda_0}$ , where  $\lambda_0$  is the wavelength of light in vacuum. In a material this becomes  $k = \frac{2\pi}{\lambda}$ , where  $n$  is the index of the refraction of the material and  $\lambda = \frac{\lambda_0}{n}$  is the wavelength of light in the material. If  $n$  is complex, then  $k$  is also complex. Since  $k$  is multiplied by  $i$  in Equation 10, a real exponent results from the complex part of  $k$ ,  $\frac{2\pi\kappa}{\lambda_0}$ . Equation 10 then becomes

$$E = E_0 e^{-\frac{2\pi\kappa}{\lambda_0} z} e^{i(-\omega t + \phi)}. \quad (11)$$

The term  $e^{-\frac{2\pi\kappa}{\lambda_0} z}$  is the damping term, which shows how much the wave is absorbed in the material.

The absorption part of the index of refraction,  $\kappa$ , causes materials to be highly absorbing in this region. Also, because the index of refraction of materials in the XUV is very close to one, light does not refract much so materials appear to be almost opaque and do not reflect well. This is also why in the XUV region one gets total external reflection only for small angles from grazing incidence.

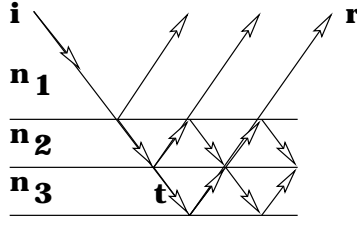


Figure 3: Multiple reflections from multilayers

Thus, if one wants a mirror to work in this region at an angle between grazing incidence and normal, it will not be possible to get much reflectivity at arbitrary angles and with one layer of material. From Equations 5 and 6 one can see that since  $n_1 \approx n_2 \approx 1$ , the Fresnel coefficients become very small and there is very little reflection. This is why one needs to use multilayer mirrors in the XUV region: there is low reflection from a single interface so with multiple layers of the right thicknesses there is constructive interference (when the waves are in phase) and the reflectivity adds. This can be seen schematically in Figure 3 as the transmitted ray in one layer is reflected off the next. Each layer in a multilayer needs to be thin, though, to reduce the amount of absorption.

Even though Fresnel's equations still hold for multilayers, it is useful to put them in a slightly different form. With multiple layers, the reflectivity of the stack can be calculated using Parratt's recursion formula [6] as cited by Kohn [5]. The discussion of reflectivity that follows is based on Kohn's work and refers to the setup in Figure 4.

The reflectivity is calculated at the midpoint of a layer in terms of the Fresnel coefficients at the boundary and the reflectivity at the midpoint of the previous layer. Equations 5 and 6 can be rewritten in terms of the wave vector  $k$  to show this. Due to Snell's law, the  $x$  components of the  $k$  vector are constant in each layer and independent of the index of refraction. This can be expressed as follows, where  $\theta$  is the angle from the normal in a vacuum and  $\lambda_0$  is the wavelength in vacuum:

$$k_x = \frac{2\pi}{\lambda_0} \sin \theta. \quad (12)$$

The  $z$  component of the  $k$  vector is different in each layer due to the transition between materials

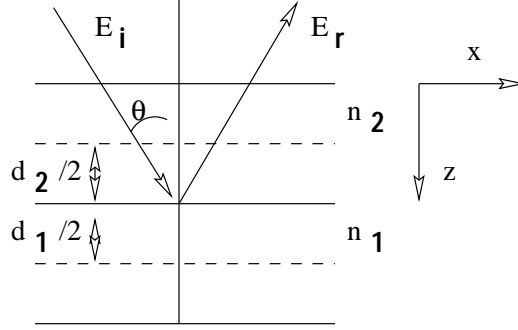


Figure 4: Geometry for the Parratt recursion formula

and changing values of  $n$ . In the following equation,  $n$  is the index of refraction for the layer:

$$k_z = \sqrt{\left(\frac{2\pi n}{\lambda_0}\right)^2 - k_x^2} \quad (13)$$

To calculate the reflectivity, the amplitude and phase of the electric field as it propagates through the layer also needs to be calculated. After a wave propagates halfway through a layer of thickness  $d$ , the phase is

$$C = e^{\frac{ik_z d}{2}}. \quad (14)$$

Written in terms of the  $k$  vector, the Fresnel coefficients become

$$r_{21}^s = \frac{k_{z2} - k_{z1}}{k_{z1} + k_{z2}} \quad (15)$$

$$r_{21}^p = \frac{n_1^2 k_{z2} - n_2^2 k_{z1}}{n_2^2 k_{z1} + n_1^2 k_{z2}}, \quad (16)$$

where  $r_{21}^s$  and  $r_{21}^p$  are the  $s$  and  $p$  coefficients, respectively, at the boundary between layers 2 and 1.

Then these coefficients can be combined with the phase to get the reflectivity for each polarization at the midpoint boundary:

$$R'_2 = \frac{C_2^4 (r_{21} + R'_1)}{1 + r_{21} R'_1}, \quad (17)$$

where  $R'_m = C^2 R_m$  and  $R_1$  is the reflection amplitude in the previous layer. At the substrate layer of the stack,  $R = 0$  since there is only a transmitted wave. Therefore, Equation 17 can be applied recursively, beginning at the bottom where  $R_1$  is known to be zero. Applying this equation repeatedly

eventually gives the reflection amplitude at the top of the stack where the vacuum thickness is taken to be zero.

In general,  $R$  is complex in the XUV region since it gives the amplitude and phase relations between the incident and reflected waves. Thus, the actual reflectivity,  $\mathcal{R}$ , at the top of the stack can be calculated as follows:

$$\mathcal{R} = |R|^2. \tag{18}$$

## 1.6 A New Application of the GA

Genetic algorithms have been used in optimization problems in fields related to multilayer mirrors and seem to produce better results than alternative methods [3]. However, they have never been used in the soft x-ray region for optimizing multilayer mirrors before, especially bifunctional mirrors.

In applying the genetic algorithm (GA), many of the parameters in the code had to be determined that are specific to the problem of designing a mirror for the IMAGE Mission. Also, each problem that the GA is applied to requires a different merit function. It took many attempts to find the merit function that best optimized the qualities of the mirror important for this mission. Even though GA's have been used in various optimization problems and the outline of the code is fairly well established, it was altered in this application by using a hybrid. A simplex algorithm was used in conjunction with the GA to cut down on the computation time. Similar approaches have been used effectively by others in different applications of the GA such as using the GA with simulated annealing in calculating the optical constants of materials [9].

## 1.7 Outline

In Section 2, the Genetic Algorithm will be explained, in general as well as its application to the mirrors for the IMAGE Mission. Section 3 will present and discuss results obtained for various applications of the GA and relate a history of the search for the best mirror design. The conclusion in Section 4 will discuss when it is useful to use the GA, some rules to apply it, and future work to

be done.

## 2 Genetic Algorithm

### 2.1 Description

As the name implies, GA's use a similar technique to nature's process for optimization and refinement through the use of DNA and survival of the fittest [3]. Table 1 describes some of the terminology used in the GA. The attributes of each member of the *population* to be optimized are encoded in a DNA-like array within *chromosomes*. For the specific problem described in Section 1.2, the materials and thicknesses in the multilayer were encoded into a *gene*, an array containing the materials and thicknesses in the stack, as shown in Figure 5. Each *allele* in the *gene* was stored in a byte so there were constraints on the thicknesses due to the storage constraints. The initial *population* of mirrors was chosen randomly with the program choosing the two materials to use and each layer thickness, with the number of layers being fixed for each run.

|            |            |                      |                      |                      |                      |
|------------|------------|----------------------|----------------------|----------------------|----------------------|
| Material 1 | Material 2 | 1 A -<br>Thickness 1 | 2 A -<br>Thickness 2 | 1 B -<br>Thickness 3 | 2 B -<br>Thickness 4 |
|------------|------------|----------------------|----------------------|----------------------|----------------------|

Figure 5: Composition of the Chromosomes

*Parents* are then selected based on the value of their merit function, which contains the information to be optimized. The merit function in this application of the GA included the specifications of the mirror design for the IMAGE Mission. *Children* are then produced by crossover and mutation of the parents' genes. The next *generation* is composed of these *children* and the best *parents* of the current *generation* with the process continuing until the merit function ceases to change significantly. A schematic of the GA is shown in Figure 6.

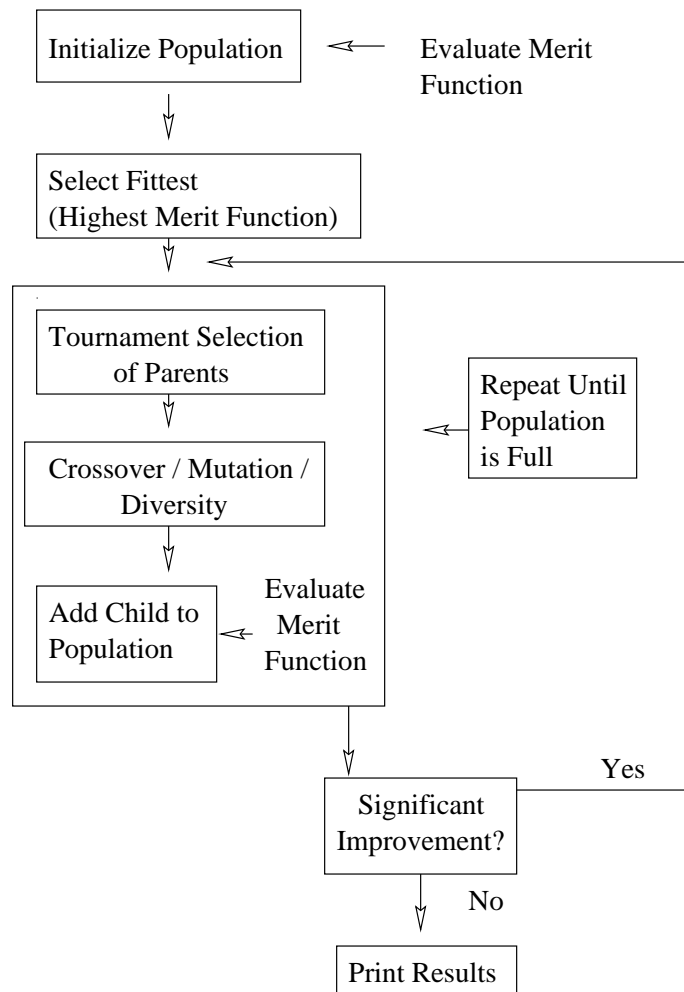


Figure 6: Flow chart of the Genetic Algorithm



|                   |  |
|-------------------|--|
| <i>Population</i> | set of trial solutions   |
| <i>Generation</i> | successively created population                                    |
| <i>Gene</i>       | array containing materials and thicknesses                         |
| <i>Allele</i>     | each material or thickness in the gene                             |
| <i>Parent</i>     | member of the current generation                                   |
| <i>Child</i>      | member of the next generation                                      |
| <i>Chromosome</i> | coded form of a trial solution consisting of genes made of alleles |

Table 1: Terminology in the GA

## 2.2 Advantages and Disadvantages for this Class of Problems

The GA is a global optimization procedure that overcomes many of the problems associated with local optimization procedures. Although this technique finds global extremes, it usually converges slowly to a solution and takes much computation time since it begins in a hit-and-miss fashion to fill the population. Despite being time intensive, one does not need to compute gradients for convergence, as in some of the local optimization techniques, so the actual encoding of the problem is quite simple. Also, global techniques are not dependent on an initial guess, a very useful feature when encountering a new problem for which one has no intuition. The GA also handles discrete variables and constraints on variables, which local optimizers do not handle well.

## 2.3 The GA Applied to the IMAGE Mission

In applying the GA to the design of mirrors for the IMAGE Mission, many parameters had to be chosen and studies done to assure that the code would find the best solution. Table 2 lists the parameters that must be chosen each time the GA is applied to a new problem.

|                                 |
|---------------------------------|
| Crossover Probability           |
| Mutation Probability            |
| Population Size                 |
| Replacement Percentage          |
| If a hybrid is used:            |
| amount of population applied to |

Table 2: Parameters specific to each application of the GA

### 2.3.1 Materials and Thicknesses

Before choosing the parameters specific to the problem, information about the problem must be encoded in the GA. Much of this is described earlier in this section. In coding the GA for the IMAGE Mission mirrors, each mirror or member of the population was allowed to have two materials with up to two oxides on top. The code allowed for the materials of the mirror to be fixed by the user or chosen from a database by the program. The database was a compilation of many common materials and included the optical constants of these materials at 304 and 584 Å's.

There were also constraints placed on the thicknesses of each layer. The alleles in the gene were each stored in a byte. This created an upper limit on the thicknesses of each layer of 255 Å which was extended to 275 Å by adding 20 Å to each thickness at the end of each run. This made the lower limit for each thickness to be 20 Å, which is a realistic lower limit on the growing capabilities of layers.

### 2.3.2 Study of Seeds

The GA was coded in C++ with the initial population randomly produced using the random number generator included in C++ and a seed chosen. The seed was important in helping to know if the population size was large enough to make sure all of the solution space was sampled. The population

size must be chosen carefully when applying the GA to a specific problem because if the population size is too small, not enough of the solution space is sampled and the best solution may be missed.

In Tables 3, 4, and 5, *Mat* and *R* refer to the materials and reflectivities at 304 Å for each seed. The data was obtained by running the GA with three different seeds. The seeds used are as follows: #1 199282721, #2 249283612, #3 847162553.

| <b>4 Layers</b> |                    |        |       |        |                      |        |
|-----------------|--------------------|--------|-------|--------|----------------------|--------|
| Population      | Mat 1              | R 1    | Mat 2 | R 2    | Mat 3                | R 3    |
| 200             | B <sub>4</sub> C/U | 12.85% | U/Se  | 17.22% | CaF <sub>2</sub> /Al | 12.86% |
| 600             | U/Te               | 20.82% | U/Te  | 20.83% | U/Si                 | 18.1%  |
| 4000            | U/Te               | 20.82% | U/Te  | 20.83% | U/Te                 | 20.83% |

Table 3: Study of 4 layer mirrors designed with different seeds

From Table 3, one can see that at a population of 4000 all three seeds gave the same result, while at a population of 200 and 600 the results are very different between the seeds. Thus, it appears that a population of 4000 is a large enough population to sample the whole solution space and not miss the best solution for a mirror with four layers.

| <b>10 Layers</b> |                                  |        |                                   |        |                                   |        |
|------------------|----------------------------------|--------|-----------------------------------|--------|-----------------------------------|--------|
| Population       | Mat 1                            | R 1    | Mat 2                             | R 2    | Mat 3                             | R 3    |
| 200              | U/Te                             | 31.73% | U/Ta                              | 12.86% | U/Ta                              | 12.86% |
| 600              | U/Te                             | 31.72% | U/Te                              | 31.73% | U/Te                              | 31.73% |
| 4000             | Al/Y <sub>2</sub> O <sub>3</sub> | 32.45% | Y <sub>2</sub> O <sub>3</sub> /Al | 33.64% | Y <sub>2</sub> O <sub>3</sub> /Al | 33.64% |

Table 4: Study of 10 layer mirrors designed with different seeds

In Table 4, the solutions are approximately equal among the seeds for a population of 4000, but it is probably not a large enough population to make sure all of the solution space is sampled since

the reflectivities differ between the three seeds by over a percent. From the results for a population of 600, it appears that that is a large enough population since the designs from all three seeds are the same. The solution is not as good, though, as that found with a larger population so the design with 600 must be a local extreme.

| 16 Layers  |                   |        |                                   |        |                                   |        |
|------------|-------------------|--------|-----------------------------------|--------|-----------------------------------|--------|
| Population | Mat 1             | R 1    | Mat 2                             | R 2    | Mat 3                             | R 3    |
| 200        | U/CH <sub>2</sub> | 17.92% | U/CH <sub>2</sub>                 | 19.16% | U/CH <sub>2</sub>                 | 19.16% |
| 600        | U/Te              | 34.03% | U <sub>3</sub> Si/Te              | 23.12% | U <sub>3</sub> Si/Te              | 23.12% |
| 4000       | U/Te              | 34.14% | Y <sub>2</sub> O <sub>3</sub> /Al | 36.42% | Y <sub>2</sub> O <sub>3</sub> /Al | 36.42% |

Table 5: Study of 16 layer mirrors designed with different seeds

Obviously, from Table 5, a population of 4000 is not large enough when optimizing a mirror with 16 layers either. If the population was large enough to sample all of the space, all three seeds would have given the same materials and approximately the same reflectivities. Since there is such a difference between the results obtained with the three seeds at a population of 600, a much larger population is probably required for a mirror of 16 layers than for one of 4 or even 10 layers to be assured that the entire solution space is sampled.

Even though seeds 2 and 3 were able to come up with a little better solution for the case of a 16 layer mirror and a population of 4000, seed 1 allowed the GA to find better solutions over all, as can be seen from Tables 3, 4, and 5, and was used in all of the succeeding calculations.

### 2.3.3 Selecting Parents and Reproduction

One of the decisions to be made in applying the GA is the selection of parents. Some strategies include: *population decimation* where only the members with merit functions above a cutoff value are kept, *proportionate selection* where the probability of choosing a parent is based on its fitness, and *tournament selection* [3]. In the application of the GA described here, several strategies were tried

but the tournament selection was chosen as it seemed to work the best. In a tournament selection, two members of the population are chosen randomly and their merit functions are compared with the higher one “winning.” This is repeated and the two “winners” then undergo crossover and mutation of a copy of their genes to produce two children.

When crossover occurs, as shown in Figure 7, a random byte (allele) in the gene is chosen and at that location, the byte becomes a hybrid of the two parents’ genes at that byte. For a discrete variable, the new allele is a combination of the bits of the parents’ allele at that point. For a continuous variable, the allele in the children becomes an average of the two parents’ alleles. The bytes before the location of the hybrid are then copied from one parent and all of those after the location are copied from the other parent. The degree to which crossover occurs is based on a crossover probability determined in encoding the GA for a specific problem. In mutation, as shown in Figure 8, a random byte is chosen in the gene and is randomly altered. The mutation probability is similar to the crossover probability in that it determine how often, if ever, the mutation is applied in producing children.

This selection of parents and reproduction is repeated until the number of children desired is produced. These children and the best members of the parent population or previous generation then make up the new generation. The percent of the previous population to be kept is one of the parameters to be chosen in each application of the GA (see Table 2).

An attempt was made to include diversity in the code to better simulate natural selection. In nature, if animals compete for the same resources, the strongest will survive by being able to get more of the food. Diversity exists in nature because different animals eat different food and do not compete with each other. In the code, multiple occurrences of a set of materials would be like animals competing for the same food. The first member in a population with certain materials was given a weight of one and all other occurrences of those materials were given a successively lower number as a weight. This weighting was then included in the reflectivity calculations, with the first instance having the highest reflectivity. By decreasing the reflectivity of multiple instances of the materials,

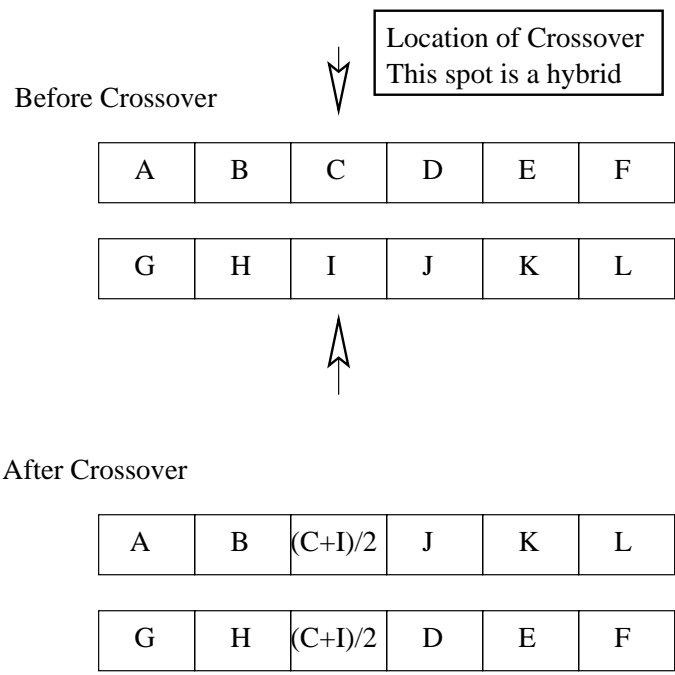


Figure 7: Crossover of the Genes

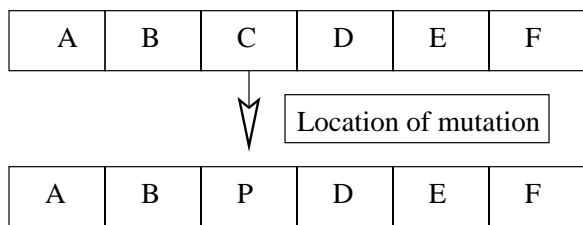


Figure 8: Mutation of the Genes

the merit function is decreased and the chances of the mirror surviving to the next generation are decreased. This diversity attempts to sample more of the solution space and get out of local minima if the code gets stuck. Unfortunately, I never got this feature working to my satisfaction.

### 2.3.4 Merit Function

The merit function in this problem compared the reflectivity of each member at 304 Å against its reflectivity at 584 Å to fit the specifications of the mirror design, as explained in Section 1.2. The merit function used follows, where  $R_{304}$  and  $R_{584}$  are the reflectivities at 304 Å and 584 Å respectively:

$$\frac{R_{304}}{\max(.002, R_{584})}. \quad (19)$$

One can see from this relation that stacks with high reflectivity at 304 Å and low reflectivity at 584 Å will be favored above other stacks by having a higher merit function and, thus, being more likely to survive in subsequent populations and to produce children. The program seemed to favor minimizing the reflectivity at 584 Å over maximizing the reflectivity at 304 Å. As a result, mirrors were found with very good low reflectivity at the longer wavelength that more than satisfied the requirements but the reflectivity at the shorter wavelength was not very high. It was more important, then to only get the reflectivity at 584 Å down to .2% and not any lower. By taking the maximum value between .2% and the reflectivity of the mirror at 584 Å when calculating the merit function, the program was forced to maximize the reflectivity at 304 Å and better mirror designs were found.

Several functions were tried before deciding to use the merit function shown in Equation 19. Since the mirror was to be highly reflective at 304 Å and non-reflective at 584 Å, the first merit function tried was:

$$\frac{R_{304}}{R_{584}}. \quad (20)$$

This function did not work very well because the code weighted the minimization of the reflectivity at 584 Å more than the maximization of the reflectivity at 304 Å. Another function tried included

the specifications of the mirror design as stated in Section 1.2:

$$\frac{R_{304}}{.2} + \left(1 - \frac{R_{584}}{.002}\right). \quad (21)$$

This function again had the problem that the minimization at 584 Å was weighted much more than the maximization at 304 Å so mirrors were found with very low reflectivity over all.

### 2.3.5 Hybrid Used

The GA uses a time-intensive hit-and-miss approach to initialize and alter each generation. To cut down on the execution time of this program and to make sure the entire solution space was sampled, the genetic algorithm (a global optimizer with slow convergence) was combined with a simplex algorithm (a local optimizer with rapid convergence). The GA was used to initialize the population and then the simplex was applied to the thickness of the mirrors to improve a certain amount of the population. In the simplex algorithm, the thicknesses of a stack are encoded into a simplex—a geometric shape representing the parameter space which is altered until the optimal solution is found [10]. The simplex was only applied to a small amount of the population (one hundredth) and it was found that this made for more rapid convergence to the optimal solution and allowed the GA to be applied to smaller population sizes without sacrificing performance.

| <b>Materials Unfixed</b> |     |                  |                  |                                   |           |
|--------------------------|-----|------------------|------------------|-----------------------------------|-----------|
| Hybrid                   | Gen | R <sub>584</sub> | R <sub>304</sub> | Mats                              | Time(sec) |
| yes                      | 14  | .2%              | 34.2%            | U/Te                              | 2763.4    |
| no                       | 3   | .2%              | 20.72%           | Y <sub>2</sub> O <sub>3</sub> /Al | 329.0     |

Table 6: 16 layers on SiO<sub>2</sub> with a population of 6000

The data in Table 6 was obtained with the GA choosing the materials for a mirror made up of 16 layers (8 layer pairs) on SiO<sub>2</sub> with a population of 6000. The GA was first run with the hybrid acting on one hundredth of the population and then as the straight GA. The GA with hybrid found



a much better solution than the straight GA, as can be seen by comparing the reflectivities at 304 Å. The computation time for the hybrid run on a DEC Alpha workstation was about nine times greater than for the run without hybrid probably because more generations were produced before a good solution was found. The straight GA run looks like it got stuck in a local maximum very early on in the run and was unable to get out. The hybrid, on the other hand, sampled more of the solution space and so was able to find a better solution.

| <b>Materials Fixed</b> |     |                  |                  |                                   |           |
|------------------------|-----|------------------|------------------|-----------------------------------|-----------|
| Hybrid                 | Gen | R <sub>584</sub> | R <sub>304</sub> | Mats                              | Time(sec) |
| yes                    | 10  | .2%              | 36.45%           | Y <sub>2</sub> O <sub>3</sub> /Al | 1967.2    |
| no                     | 41  | .2%              | 36.23%           | Y <sub>2</sub> O <sub>3</sub> /Al | 4019.0    |

Table 7: 16 layers on SiO<sub>2</sub> with a population of 6000

The data in Table 7 was obtained by running the GA with the materials fixed to see how the two versions of the program compared. This study shows the difference in the computation time between the GA with hybrid and without. From the time of computation and the number of generations taken, one can see that the hybrid was able to converge to a solution much quicker than the regular GA. It looks like each generation of the regular GA takes less computation time, though, which is very surprising. Although the simplex algorithm converges to a solution faster than the GA does, it requires more iterations for each step so it may sometimes actually take longer to find a good solution than the GA, as in Table 6.

There are many other local optimizers that could have been used in conjunction with the GA in this application, such as conjugate gradient or BCGS. The simplex is probably the slowest local optimizer known but it is also the most robust and easiest to implement.

### 3 Results

A discussion is given of the results obtained using the GA for the IMAGE Mission and the mirror design actually used for the IMAGE project in Section 3.1. A history of the search for the best design is given in Section 3.2. Section 3.4 describes another application of the GA that arose while working on the mirrors for the IMAGE Mission. In Section 3.3, a description is given of a study of the experimental methods used in designing and making the mirrors. The values of the parameters used in this application are given in Section 3.5.

#### 3.1 Mirrors Designed for the IMAGE Mission

In searching for the optimal design of the mirror for the IMAGE Mission, the GA was run with the following specifications: hybrid, 16 layers, mutation probability=0.05, crossover probability=0.75, population size=8000, replacement percentage=50%, and the program was allowed to choose the materials. The best design found was  $\text{Y}_2\text{O}_3/\text{Al}$  with a reflectivity at  $304 \text{ \AA}$  of 36% and a reflectivity at  $584 \text{ \AA}$  of  $< .02\%$ , as shown in Figures 9 and 10.

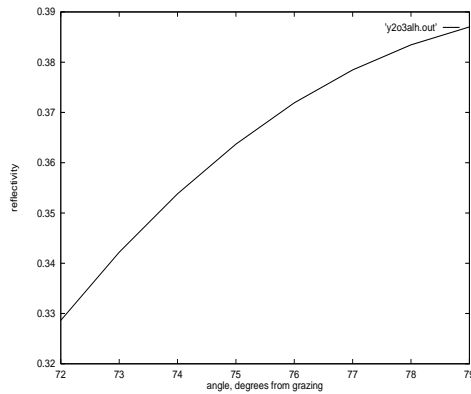


Figure 9: Reflectivity of  $\text{Y}_2\text{O}_3/\text{Al}$  at  $304 \text{ \AA}$ .

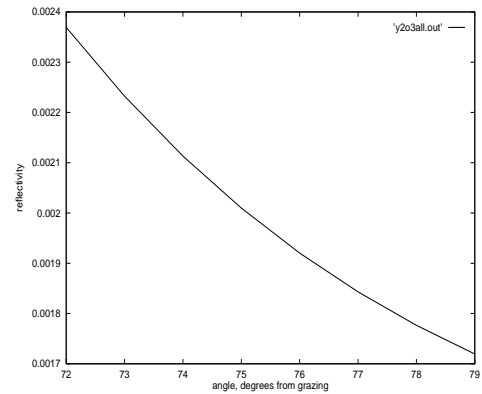


Figure 10: Reflectivity of  $\text{Y}_2\text{O}_3/\text{Al}$  at  $584 \text{ \AA}$ .

This design was very surprising and non-intuitive because it included an oxide. The presence of oxygen in the form of an oxide on the top of a mirror usually decreases the reflectivity significantly.

Also, elements were thought to reflect better than compounds. This mirror design seemed better than other designs from an experimental view, though, since it already includes an oxide. Most mirrors are made and then the top layer or so oxidizes and the reflectivity decreases because oxygen has a very low index of refraction. The  $Y_2O_3/Al$  mirror would not have that problem since the Y is already in an oxide compound.

Attempts were made to grow the  $Y_2O_3/Al$  mirror but many difficulties were encountered. Due to the nature of  $Y_2O_3$ , a ceramic, the sputtering process used at the time to produce the mirrors would not work. An RF power supply was needed to deposit this ceramic but the process was not worked out within the time constraints so other designs were used.

The next multilayer mirror design tried was U/Al, but these materials oxidize too quickly, especially Al. Thus, U/Si was used for the mirror for the IMAGE Mission with a layer of U placed on top to oxidize. This design was much more practical than  $Y_2O_3/Al$  and the U and Si targets were already available and those fabricating the mirrors had had experience with sputtering them. The design for the mirror made for the project was that it be a periodic U/Si multilayer with 7 layer pairs or 14 layers total and a thin layer (39.7 Å) layer of  $UO_3$  on top. The thickness for each U layer was to be 53.6 Å and for the Si layers was to be 128.5 Å.

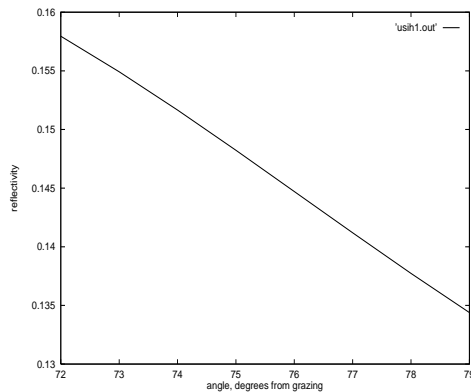


Figure 11: Reflectivity of U/Si at 304 Å.

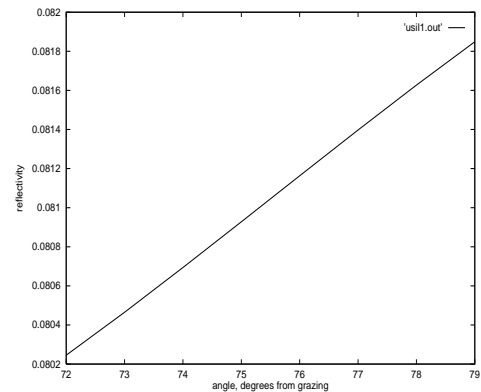


Figure 12: Reflectivity of U/Si at 584 Å.

It was surprising that the mirror that was made to these specifications reflected better than the theoretical design did. Some possible reasons for this discrepancy are given in Section 3.3. At 304 Å the high reflectivity was 17% and the reflectivity at 584 Å was .84%. This is much different than the theoretical reflectivities at both wavelengths. At 304 Å the theoretical reflectivity was about 15% while at 584 Å it was about 8%. The actual makeup of the mirror was determined to be the same as what was desired through x-ray diffraction. The U cap placed on top of the mirror was designed to completely oxidize and to protect the layers underneath from oxidation which would decrease the reflectivity.

### 3.2 Periodic and Aperiodic Designs

When this project was begun, it was unknown which materials would be best to use for the mirrors. A study was first done of Mo/Si periodic stacks at 584 Å with variable periods. The substrate was SiO<sub>2</sub> for all of the calculations. The best results found using a program called fit2, written by members of the group working on this project, was a three-period stack with the Mo layers 162 Å thick and the Si layers 372 Å thick. This design had a reflectivity of 23% at 584 Å.

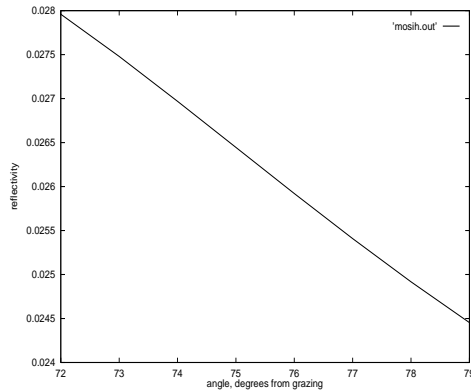


Figure 13: Reflectivity of Mo/Si at 304 Å.

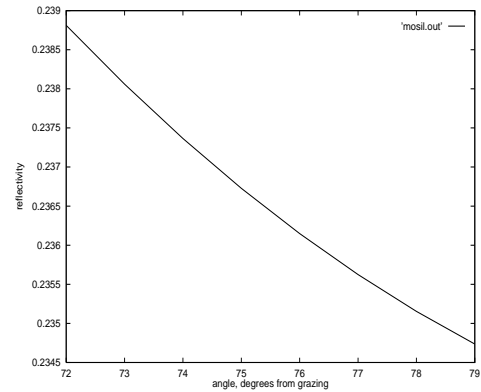


Figure 14: Reflectivity of Mo/Si at 584 Å.

Figures 13 and 14 show that this stack was much more reflective at 584 Å than at 304 Å. This

follows what is known about materials in the XUV region, that most materials are more reflective at 584 Å than at 304 Å, which made the project very difficult. Many multilayer mirror applications use mirrors made of Mo/Si, but the goal is usually just to achieve high reflectivity at one wavelength and not to produce a bifunctional mirror, with high reflectivity at one wavelength and low at another.

Some of the first materials tried for the design of the mirror were U and Al. A study was conducted of U/Al periodic stacks and then aperiodic stacks to see how they compared. With a periodic stack, the best design found using a program by David Windt called IMD had a reflectivity of about 20% at 304 Å and about .5% at 584 Å as shown in Figures 15 and 16. The stack was composed of eight periods of U with a thickness of 41 Å and Al with a thickness of 129 Å on SiO<sub>2</sub>.

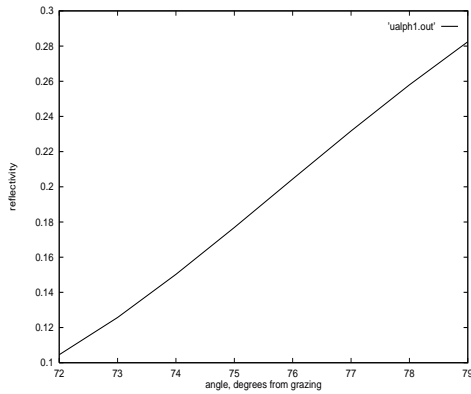


Figure 15: Reflectivity of periodic U/Al at 304 Å.

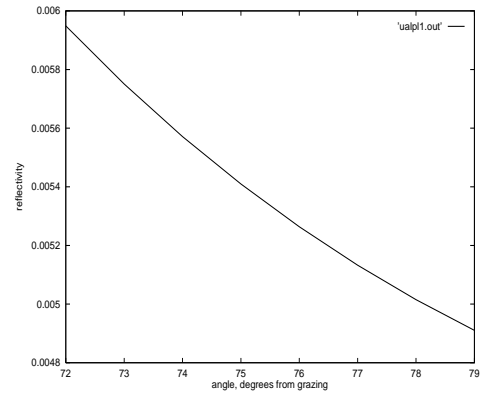


Figure 16: Reflectivity of periodic U/Al at 584 Å.

A better stack was found with an aperiodic design. The aperiodic stack was made of sixteen layers total or eight pairs of U/Al on SiO<sub>2</sub>. This stack had a reflectivity of 32.69% at 304 Å and approximately 1% at 584 Å as shown in Figures 17 and 18.

At the same time, studies were also conducted with U/Si stacks and Al/U and Si/U stacks with various oxides on the top to simulate reality. The data from these stacks was not very encouraging as designs that fit our specifications were not found.

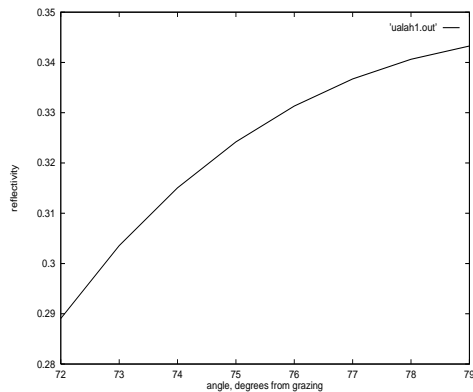


Figure 17: Reflectivity of aperiodic U/Al at 304 Å.

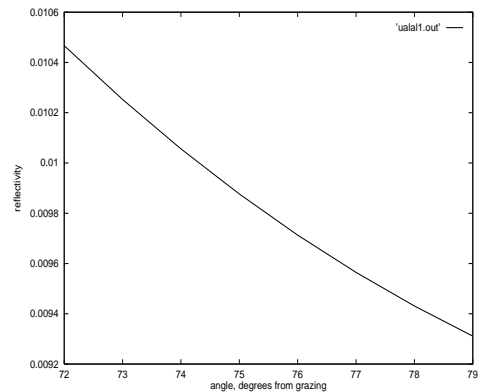


Figure 18: Reflectivity of aperiodic U/Al at 584 Å.

There was some concern about the oxidation of the materials being used in the designs and also with the use of uranium. Uranium is radioactive in large amounts and even in the small amounts present in the mirrors there was some concern that it would give off counts that would obscure the detection of He-II. These concerns about materials and the difficulty in using local optimization techniques led to the application of the GA to this problem.

### 3.3 Diagnostics

It was found that when mirrors were grown to the theoretical specifications found by the GA that the reflectivities were vastly different than were proposed. The results obtained using the GA were checked using IMD and fit2 and the reflectivities matched if the same optical constants were used. This led to a study of how reflectivity changed with thickness to see if the actual makeup of the mirrors could be determined. The focus was on finding a minimum in reflectivity at about 584 Å and studying how changes in thickness moved this minimum. Unfortunately, the studies were conducted for multilayers with Si on U but the mirrors were grown with U on Si. As a result, this information did not reveal anything.

Although, the study did not work, there are some ideas of the causes of incorrect thicknesses in the mirrors made. This could be caused by using wrong optical constants. In the XUV region, there are many discrepancies in the optical constants among different sources. Roughness could also account for the difference between the theoretical and experimental designs as it was not taken into account in the theoretical calculations. From analysis of some of the layers, it is apparent that there is diffusion between the layers and the interfaces between the two materials are not abrupt. This changes the makeup of the mirror and, thus, affects the reflectivity. From Figures 11 and 12, it is apparent that the theoretical design was sometimes not as good as the experimental design. This could be due to errors in the program.

### 3.4 Polarizers

The GA has been applied to the design of polarizers, as well, by members of the research group. All light has two polarizations called  $s$  and  $p$  as shown in Figure 2. A polarizer will transmit or reflect one of these polarizations better than the other. Thus, a good polarizer will be such that the reflective ray is almost all  $s$  or  $p$ —known as linear polarization. The merit function used in this application of the GA is the average of the  $s$  and  $p$  polarization, known in the literature as the extinction coefficient:

$$\frac{R_s}{R_p}. \tag{22}$$

### 3.5 Selection of Parameters

The GA depends on the choice of the following adjustable parameters: the crossover probability, the mutation probability, the replacement percentage, the population size, the merit function, and how much of the population the hybrid is applied to. These parameters were studied for the problem discussed in this paper to see what the optimal values were. The results are shown in Section 3.5.2.

### 3.5.1 Study of Population Size (N)

As can be seen from Tables 8, 9, and 10, the GA was able to produce many different mirror designs which meet the specifications at 584 Å and exceed the specifications at 304 Å. To get the following results, GA was run with hybrid acting on one hundredth of the population, seed #1, crossover probability=0.75, mutation probability=0.05, and replacement=50%. In the tables, *Population* is the size of the population, *Gen* is the number of generations used to get the solution, and  $R_{584}$  and  $R_{304}$  are the reflectivities at the two wavelengths in Å.

| 4 Layers   |     |           |           |                      |           |
|------------|-----|-----------|-----------|----------------------|-----------|
| Population | Gen | $R_{584}$ | $R_{304}$ | Mats                 | Time(sec) |
| 200        | 5   | .2%       | 12.86%    | CaF <sub>2</sub> /Al | 7.9       |
| 500        | 6   | .2%       | 11.87%    | CaF <sub>2</sub> /Al | 23.1      |
| 1000       | 8   | .2%       | 20.82%    | U/Te                 | 51.0      |
| 2000       | 6   | .2%       | 20.83%    | U/Te                 | 91.1      |
| 4000       | 6   | .2%       | 20.83%    | U/Te                 | 180.7     |
| 8000       | 4   | .2%       | 20.83%    | U/Te                 | 235.9     |

Table 8: Study of 4 layer mirrors with different populations

If the population is too small, the best solution is often missed as not enough of the solution space is being sampled. This can be seen in the Tables 8, 9, and 10, where the Y<sub>2</sub>O<sub>3</sub>/Al solution was only found with a large population. In Table 9, a population of 8000 allowed a better solution to be found than at 16000. This means that a population of 16000 is not large enough when optimizing a mirror of 10 layers to ensure that the best solution is found. The solution being better with the smaller population in this instance is mainly due to the randomness of the GA; the initial population is randomly generated and altered.

The time of computation depends on the population size and the number of generations needed to



| 10 Layers  |     |                  |                  |                                     |           |
|------------|-----|------------------|------------------|-------------------------------------|-----------|
| Population | Gen | R <sub>584</sub> | R <sub>304</sub> | Mats                                | Time(sec) |
| 200        | 14  | .2%              | 21.75%           | USi <sub>2</sub> /Te                | 75.9      |
| 500        | 11  | .2%              | 28.18%           | U/AlSi                              | 118.4     |
| 2000       | 8   | .2%              | 31.72%           | U/Te                                | 420.7     |
| 4000       | 9   | .2%              | 31.96%           | Y <sub>2</sub> O <sub>3</sub> /AlSi | 944.3     |
| 5000       | 9   | .2%              | 31.96%           | Y <sub>2</sub> O <sub>3</sub> /AlSi | 941.5     |
| 6000       | 9   | .2%              | 31.96%           | Y <sub>2</sub> O <sub>3</sub> /AlSi | 1129.9    |
| 8000       | 12  | .2%              | 33.63%           | Y <sub>2</sub> O <sub>3</sub> /Al   | 1980.0    |
| 12000      | 7   | .2%              | 31.73%           | U/Te                                | 2135.2    |
| 16000      | 7   | .2%              | 31.73%           | U/Te                                | 2838.3    |
| 20000      | 11  | .2%              | 33.65%           | Y <sub>2</sub> O <sub>3</sub> /Al   | 4694.0    |

Table 9: Study of 10 layer mirrors with different populations

converge to a solution. By comparing those runs with similar numbers of generations, a comparison can be made of the change in computation time due to an increase in population, as all of this data was found by the GA running on a DEC Alpha workstation. Most optimization procedures use powers of  $N$  iterations, where  $N$  is the population size. With an optimizer that scales like  $N^2$ , a population of 1000 will have  $1000^2$  iterations. If the population is then increased to 4000, 4 times larger, the number of iterations is increased to  $4000^2$ , or 16 times larger. As can be seen from Tables 8, 9, and 10, the GA is fairly linear with relation to time. Thus, increasing the population by large amounts will not increase the computation time very much.

The number of generations in the calculations affects the running time as well. This is why in Table 10 the running time for a population of 2000 was larger than for a population of 4000. Figure 19 shows the convergence of the GA. If a good solution is found very quickly but small

| <b>14 Layers</b> |     |                  |                  |                                     |           |
|------------------|-----|------------------|------------------|-------------------------------------|-----------|
| Population       | Gen | R <sub>584</sub> | R <sub>304</sub> | Mats                                | Time(sec) |
| 200              | 13  | .2%              | 25.19%           | USi <sub>2</sub> /Te                | 96.7      |
| 500              | 19  | .18%             | 30.11%           | U/AlSi                              | 276.6     |
| 2000             | 26  | .2%              | 33.69%           | U/Te                                | 1532.6    |
| 4000             | 10  | .2%              | 33.77%           | Y <sub>2</sub> O <sub>3</sub> /AlSi | 1145.7    |
| 5000             | 13  | .2%              | 33.81%           | Y <sub>2</sub> O <sub>3</sub> /AlSi | 1873.8    |
| 6000             | 18  | .2%              | 35.9%            | Y <sub>2</sub> O <sub>3</sub> /Al   | 3095.0    |
| 8000             | 12  | .2%              | 33.71%           | U/Te                                | 2727.9    |
| 12000            | 11  | .2%              | 35.85%           | Y <sub>2</sub> O <sub>3</sub> /Al   | 3803.8    |
| 16000            | 13  | .2%              | 35.89%           | Y <sub>2</sub> O <sub>3</sub> /Al   | 5938.4    |
| 20000            | 12  | .2%              | 35.91%           | Y <sub>2</sub> O <sub>3</sub> /Al   | 8729.7    |

Table 10: Study of 14 layer mirrors with different populations

changes are still made for many generations, the running time may be much longer than is actually needed. This shows one of the aspects of the GA that still needs to be worked on.

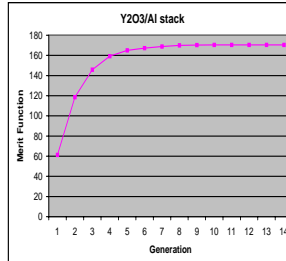


Figure 19: Convergence of GA.

### 3.5.2 Optimal Parameters

For each application of the GA to a different problem, one must find the optimal values for certain parameters used in the code. The main parameters to be chosen are the amount of each population that is replaced by new children, the crossover probability, and the mutation probability. If a hybrid is used, one must also choose the amount of each population to apply the hybrid to. Each problem also requires its own merit function specific to what is being optimized. Johnson and Rahmat-Samii [3] give a range of values in which the optimal solution for most problems will be found: smaller replacement percentages usually lead to faster convergence, 0.6-0.9 for the crossover probability, and 0.01-0.1 for the mutation probability. For the problem of finding a mirror that is highly reflective at  $304 \text{ \AA}$  and non-reflective at  $584 \text{ \AA}$ , the best values for the parameters listed above were found to be: replacement percentage=50%, crossover probability=0.7, mutation probability=0.05, and the hybrid applied to the population divided by 100.

## 4 Conclusion

### 4.1 Where the GA is Valuable

In doing optimization, it is useful to have a technique that finds a global extreme and not just a good solution. Unfortunately, there is not a perfect procedure for optimization. One must weigh the pros and cons of the local and global techniques and decide which features are most beneficial.

The GA is useful in optimization problems where one has no idea what the solution will look like. It also is very useful when satisfying many different parameters and when the problem has discrete parameters and discontinuities. The random nature of this algorithm allows more of the solution space to be sampled and, if the population is large enough, to find the global extreme and not get stuck in a local extreme. This feature makes the GA inherently time intensive, though.

In designing a mirror to meet the specifications of the IMAGE Mission, a hybrid approach worked best—the GA to find solutions all over the parameter space and a simplex algorithm to converge to the best solution. This hybrid significantly reduced the computation time and allowed smaller populations to be used without sacrificing the optimal solutions.

### 4.2 Rules for Application of the GA

When applying the GA to any problem, there are many parameters to be chosen: the population size, the mutation and crossover probabilities, the amount of each generation to be kept, and the merit function. Also, if time is a concern, a hybrid with another algorithm should be used. If a hybrid is used, one must decide how much of each generation to apply it to. For the problem of finding a mirror that was highly reflective at 304 Å and non-reflective at 584 Å, the following parameters were found to work best: crossover probability=0.7, mutation probability=0.05, replacement percentage=50%, and the hybrid was applied to one-hundredth of each generation (population/100).

### 4.3 Future Research

More work still needs to be done on this application of the GA before it is complete. Currently, the GA only optimizes aperiodic stacks; it allows each layer to be a different thickness. The code needs to be altered to optimize periodic stacks as well. In this case, the GA would probably not be much better than traditional local optimization techniques due to its random nature, but it would run faster than with the problem described in this paper because there would be fewer parameters.

The code used in this optimization also did not take into account manufacturability or feasibility of a design. There was a feature built in that would weight different materials more than others to represent lower cost or easier manufacturing but this feature was never fully developed or used. Also, the code is designed to optimize a mirror for broadband reflectivity. This can be changed with minimal altering of the code but the merit function may need to be changed as well.

There were also many problems with getting the calculated and measured reflectivities to match. This is probably due to the uncertainty in optical constants in the XUV region. Many sources have vastly different values for  $n$  and  $\kappa$  so it was difficult to know which to use. Also, for many wavelengths in the XUV, the index of refraction is not even known. Obviously, this region in the spectrum still has many interesting problems that need to be studied to increase understanding of the XUV region and help the theory come closer to reality.

## References

- [1] Ethan A. Merritt, *The Kramers-Kronig Equation*, 1996, Online posting, [http://brie.bmsc.washington.edu/scatter/AS\\_kk.html](http://brie.bmsc.washington.edu/scatter/AS_kk.html), 30 Jan 1999.
- [2] Eberhard Spiller, *Soft X-Ray Optics*, Bellingham WA, SPIE Optical Engineering Press, 1994.
- [3] J. Michael Johnson and Yahya Rahmat-Samii, "Genetic Algorithms in Engineering Electromagnetics," *IEEE Antennas and Propagation Magazine*, 39, Aug 1997, pp. 7-21.
- [4] Masaki Yamamoto and Takeshi Namioka, "Layer-by-layer design method for soft-x-ray multilayers," *Applied Optics*, 31, Apr 1992, pp. 1622-1630.
- [5] V. G. Kohn, "On the theory of reflectivity by an x-ray multilayer mirror," *Phys. Stat. Sol. (b)*, 187, 1995, pp. 61-70.
- [6] L. G. Parratt, "Surface Studies of Solids by Total Reflection of X-Rays," *Physical Review*, 45, 1954, p. 359-369.
- [7] Grant R. Fowles, *Introduction to Modern Optics*, New York, Dover Publications, Inc., 1975.
- [8] T. Boudet, P. Chaton, L. Herault, G. Gonon, L. Jouanet, and P.Keller, "Thin-film designs by simulated annealing," *Applied Optics*, 35, 1996, pp. 6219-6226.
- [9] Aleksandra B. Djurišić, Joven M. Elazar, and Aleksandar D. Rakić, "Simulated-annealing-based genetic algorithm for modeling the optical constants of solids," *Applied Optics*, 36, 1997, pp. 7097-7103.
- [10] William H. Press, et. al, *Numerical Recipes in C: the Art of Scientific Computing*, New York, Cambridge University Press, 1992.